OBSERVED AND PREDICTED GROUND DEFORMATION - MILLER FARM LATERAL SPREAD, WATSONVILLE, CALIFORNIA

Thomas L. Holzer, John C. Tinsley, III, Michael J. Bennett, and Charles S. Mueller

U.S. Geological Survey
345 Middlefield Road
Menlo Park, CA 94025

ABSTRACT

Following the 1989 Loma Prieta, California, earthquake, ground deformation and subsurface conditions were carefully mapped and documented at the east end of a 1.7-km-long lateral spread south of the Pajaro River near Watsonville, California. The lateral spread occurred in natural floodplain deposits that fill a former river channel. Penetration data from geotechnical soundings and correlations of median grain size of sand boils with potential source beds at the east end of the spread indicate that a 6.1-m-thick layer, 4.6 m below the land surface, liquefied Horizontal extension across ground cracks in the study area ranged from 117 to 160 mm. Settlements ranged from 50 to 240 mm. Empirical predictions of horizontal displacements overpredict observed displacements. Empirical predictions of vertical displacements underpredict observed settlements. We conclude that the lateral spread was a deformation failure, which resulted from transient inertial forces, as contrasted with a flow failure. We also devise a test to establish the maximum displacement by a deformation failure mechanism.

INTRODUCTION

Prediction of horizontal displacement associated with liquefaction poses a significant engineering challenge. Progress has been slowed by uncertainty about potential mechanisms of lateral spreading and a shortage of well-documented field examples. The National Research Council (1985) proposed two mechanisms of lateral spreading: flow and deformation failures Flow failure occurs by continuous deformation when static gravitational forces exceed the strength of the soil after the strength has been degraded by cyclic loading or pore pressure increase. Deformation failure occurs incrementally when the combined earthquake-induced cyclic and free-field stresses momentarily exceed the resistive strength of the soil mass. The potential for deformation failure is enhanced when liquefaction decouples the surficial soil layer from the underlying nonliquefied soil. As a result of the uncertainty about failure mechanisms, current efforts to predict ground deformation have emphasized case histories and empirical correlations of displacement with site characteristics.

The purposes of this study are: (1) to describe ground deformation within part of a lateral spread that was caused by the October 17, 1989, Loma Prieta, California, earthquake (moment magnitude 6.9), and (2) to compare observed deformation to that predicted by conventional geotechnical methods. The spread, which was near Watsonville, California (Fig. 1), was one of more than 47 lateral spreads that were caused by the Loma Prieta earthquake in the region south of the epicenter (Tinsley and Dupré, 1992) It occurred in floodplain deposits near the Pajaro River. Ground deformation was well exposed in agricultural fields. Following the earthquake, we measured vertical offsets and openings across cracks and surveyed the post-earthquake topography of part of the lateral spread. Comparison of the pre- and post-earthquake topography permitted computation of settlements. In addition, we did 25 cone penetration tests (CPT) and 11 standard penetration test (SPT) borings to characterize the geologic setting and the geotechnical properties of underlying deposits.

LATERAL SPREADING

The lateral spread that we investigated was near the Pajaro River (Fig. 1). South of the river, an approximately 0.2-m-high head scarp could be followed for 1.7 km. The scarp, which undulated in map view, roughly paralleled the river channel. The scarp extended approximately 200 m from the channel, and intersected the channel at its western and eastern ends. Maximum horizontal displacement was approximately 300 mm just west of the study area. Lateral spreading also occurred on the north side of the river, but the head scarp was discontinuous; maximum horizontal displacement there was also approximately 300 mm. Ground deformation on both sides of the river was restricted to the floodplain that is now protected from flooding by man-made flood-control levees. The channelward sense of displacement across the head scarps suggested that lateral spreading on both sides of the river was toward the modern river channel, but nowhere did we see the toe of the lateral spread. Compression of two river bridges, however, suggested that lateral deformation extended into the channel area. The regional downstream slope of the floodplain inferred from the USGS Watsonville East 7½' quadrangle was approximately 0.1 per cent, but land slopes within the floodplain are substantially modified by regrading for irrigation. Before the earthquake, some fields that were subsequently damaged by the lateral spread gently sloped toward the river whereas others sloped away from the river

Sand boils provided direct evidence of liquefaction. At the eastern end of the lateral spread south of the river, the focus of our investigation, sand boils were restricted to the area affected by lateral spreading At the western end of the lateral spread, sand boils vented south of, and outside, the head scarp of the lateral spread. Eyewitnesses reported that sediment-laden water flowed gently from vents on the lateral spread during the earthquake and continued to flow for 10 to 20 minutes after the earthquake

Our investigation concentrated on the eastern end of the lateral spread with particular emphasis on the south side of the river at Clint Miller Farms. This area will be referred to herein as Miller Farm. We also conducted a less extensive investigation on the north side of the river across from Miller Farm. This area will be referred to as Farris Farm.

GEOLOGY

Before construction of flood control levees next to the Pajaro River, flooding deposited a complex interbedded sequence of fluvial deposits. Two Holocene fluvial deposits, older flood-plain deposits (Q_{of}) and younger flood-plain deposits (Q_{yf}) (Fig. 1), which are distinguished primarily based on soil development and geomorphic and stratigraphic position, were mapped in the area (Dupré and Tinsley, 1980). Areas underlain by younger flood-plain deposits are commonly topographically lower and subject to more frequent flooding than areas underlain by older flood-plain deposits.

Lateral spreading at both Farris and Miller Farms was restricted to the area underlain by the younger flood-plain deposits. In fact, the head scarp coincided with the mapped contact between the younger and older flood-plain deposits (Tinsley and Dupré, 1992). The younger flood-plain deposits fill an old river channel. The base of the younger flood-plain deposits consists primarily of point bar and channel sands. This is illustrated in Figure 2, which shows in map view the percentage of the total section in the depth interval from 4.6 to 9.1 m that consists of sand layers at each of our soundings. Sand layers were identified in CPT soundings based on friction ratio (<0.5%) and tip resistance (>3 MN/m²). As will be described in the section on liquefaction susceptibility, this interval includes most of the zone that liquefied during the Loma Prieta earthquake. Sand-layer percentages in this depth interval in the area underlain by the younger flood-plain deposits range from 67 to 100%, whereas sand-layer percentages in the area underlain by the older flood-plain deposits range from 0 to 27%. Sand in the sandy layers of the younger flood-plain deposits coarsens downward, increasing from fine to medium grained (Fig. 3). Average fines content of the sandy layers is 15%, but ranges from 22% at Miller Farm to 8% at Farris Farm. The older flood-plain deposits are predominantly clay and silt.

The upper 4.6 m of the younger flood-plain deposits is silty and generally contains only a few thin sand layers. Sand-layer percentages in this interval are shown in Figure 2 and range from 0 to 100. There also is an areal variation in the presence of sand layers in the upper interval. Sand-layer percentages in the upper 4.6 m are higher at Miller Farm than at Farris Farm.

The contact between the older and younger flood-plain deposits is sharp and presumably is erosional in origin. The sharpness of the contact can be seen vertically in most CPT soundings and also can be inferred laterally by comparing closely spaced CPT soundings that span the contact as mapped at the surface (Fig. 4). Soundings 2 and 3, which span the contact south of the river, are 79 m apart; soundings 61 and 62, which span the contact on the north side of the river, are 46 m apart. In soundings 3 and 61, which are in the area underlain by younger flood-plain deposits, an abrupt change in stratigraphy occurs at depths of 8.5 and 10.2 m, respectively. Above these depths, a thick sand body, which has a decreasing upward CPT tip resistance, is identifiable. The underlying sequence consists of finely interbedded deposits.

The buried channel is shown in cross section in Figure 5 The thickness of the younger flood-plain deposits varies, but may be as large as 14.5 m at sounding 6 (Fig. 1). The base of the younger flood-plain deposits as inferred from individual soundings at some locations was not clearcut. The underlying older flood-plain deposits locally contain sandy facies that cannot always be texturally distinguished from sands in the younger deposits. Thus, the contact that we identified in the soundings as the boundary between older and younger flood-plain deposits is provisional pending the availability of age dates for these units.

The depth to the water table was 4.6 m 10 days after the mainshock in a hand-augered boring. Most of our geotechnical soundings were conducted the following spring and yielded comparable water depths. The Pajaro River channel was dry during this period because of drought conditions. The water table at the site is probably controlled by river stage.

MAINSHOCK GROUND MOTION

The closest strong motion accelerograph that recorded the Loma Prieta earthquake mainshock is in a four-story building in Watsonville (Fig. 6). The building is 1 km west of Miller Farm and is instrumented with 13 accelerometers (See insert in Fig. 1). Peak horizontal ground-level acceleration recorded in the building was 0.39 g (Shakal and others, 1989). Strong ground shaking lasted for approximately 6 seconds. Comparison of aftershock recordings from portable instruments on the lateral spread south of the river and in the building indicates that site response on the lateral spread is similar to that at the Watsonville building location. The building sits on older flood-plain deposits outside the area that liquefied. Although the Watsonville building recording is not free field, the building is square and rests on a spread footing which suggests that soil-structure interaction probably did not greatly affect the ground-level recording (C.B. Crouse, oral commun., 1994). In addition, the mainshock ground-level peak acceleration in the building is near the median value of free-field sites on similar soils that recorded the Loma Prieta earthquake at comparable distance. A comparison of roof- and ground-level records suggests that the building is excited at 3 Hz (M. Çelebi, written commun., 1994). The ground-level peak acceleration occurs at approximately 4 Hz. The comparison also indicates that the building does not affect ground-level shaking at frequencies less than 2 Hz, which control ground displacement. Thus, we assume that the Watsonville recording closely approximates mainshock ground motion at Miller Farm.

LIQUEFACTION SUSCEPTIBILITY

The sand deposits, which fill the old channel, are heterogeneous. Corrected blow counts, $(N_1)_{60}$, vary from 7 to 28 and increase with depth. Average values for both Miller and Farris Farms are shown in Table 1. Liquefaction resistance as a function of depth beneath the lateral spread is shown in Figure 7. Both induced cyclic stress ratio and liquefaction resistance, which was determined from SPT blow counts, were computed using the simplified procedure (Seed and others, 1985). Comparison of induced cyclic stress ratios to liquefaction resistance indicates that liquefaction occurred primarily in the 6.1-m-thick sand interval from 4.6 to approximately 10.7 m. Below 10.7 m, the overall liquefaction resistance is higher although SPT tests indicate some liquefaction may have occurred below 10.7 m. The interval that is inferred to have been the primary zone of liquefaction also is consistent with the sand boils that vented at Miller Farm. The median grain sizes, d_{50}, of sand boils are shown as inverted triangles on the abscissa in Figure 3. The d_{50}'s of sand boils and the samples from the deposit from 4.6 to 10.7 m are comparable. The larger d_{50}'s of the sands below 10.7 m appear to preclude that sand boils originated from the

deeper part of the deposit.

Although sand boils and ground deformation were restricted to the area underlain by the younger flood-plain deposits, low blow counts in sandy parts of older flood-plain deposits indicate that some parts of it may have liquefied. The thinness and small number of sand layers within the area of older flood-plain deposits at Miller and Farris Farms may have masked surface manifestations of liquefaction if these layers did indeed liquefy.

OBSERVED GROUND DEFORMATION

Horizontal displacements of the land surface at Miller and Farris Farms were measured by summing openings across cracks near head scarps. Horizontal displacements measured in two profiles across the head scarp at Miller Farm were 117 and 160 mm. The profile that yielded 117 mm of horizontal displacement across the head scarp is shown in Figure 8. We also measured 454 mm of extension in this profile across the levee south of the river. We assume, however, that this extension was associated with a bearing capacity failure of the levee as it settled into underlying liquefied soil. Scarps in the levee faced inward toward the crown of the levee (Fig. 8). Extension across one crack at Farris Farm equalled 300 mm, but most of the ground cracking at Farris was affected by a bearing capacity failure of the levee on the north side of the river.

Changes of elevation of the land surface above the lateral spread at Miller Farm were estimated by comparing post- and pre-earthquake topography. Losses of elevation ranging from 50 to 240 mm are estimated in the area affected by lateral spreading (Fig. 9). The profiles indicate that the loss in surface elevation extended over the whole body of the lateral spread, but was greatest in a 30-m-wide zone at the base of the head scarp.

The post-earthquake topography was surveyed in the eastern part of the study area with a combined electronic precision theodolite and electronic distance meter. Pre-earthquake topography was computed from grading specifications provided by the land owner (Fig. 1). Before the earthquake, fields had been carefully graded for irrigation purposes by a laser-controlled grading system. The system can produce gradients at 0.02m/1000m in precision in fine-textured loose soil. To estimate pre-earthquake topography in the area affected by lateral spreading, we projected the land slope determined from grading specifications into the disturbed area from the unaffected area south of the head scarp. Note that the measured post-earthquake land slope in the undisturbed area compares favorably to the pre-earthquake graded slope reported by the landowner (Fig 9).

PREDICTED GROUND DEFORMATION

Horizontal Displacements

Several empirical methods have been proposed to predict horizontal displacements associated with lateral spreading. The most straightforward method, because it does not involve

site characterization, is described by Youd and Perkins (1987) who proposed a Liquefaction Severity Index (LSI) that provides an upper bound to horizontal displacements on fluvial sites. LSI is predicted only by earthquake moment magnitude (M_w) and distance from the fault (R).

$$\log (LSI) = - 3.49 - 1.86 \log R + 0.98 M_w \quad (1)$$

Hamada and others (1986) used observations of lateral spreading in two earthquakes in Japan to develop a correlation between displacements (D) and thickness of the liquefied interval (H) and average slope (θ).

$$D = 0.75 H^{0.50} \theta^{0.33} \quad (2)$$

Hamada (1992) and Pease and O'Rourke (1993) concluded that the best predictor of displacement is liquefied thickness. Including slope did not materially improve their predictions. Pease and O'Rourke (1993) derived the following regression for displacement with liquefied thickness (H) of fills for the 1906 San Francisco, California, earthquake, which they estimated had a peak acceleration, 0.4 g, comparable to Miller Farm.

$$D = 0.32 H + 0.14 \quad (3)$$

Bartlett and Youd (1992) compiled case histories of lateral spreads in earthquakes in Japan and the United States. They correlated displacements (D) with earthquake moment magnitude (M_w), horizontal distance to seismic source zone (R), slope (θ) or the ratio of the height of the free face to the distance of lateral spreading from the free face (W), and the thickness (H), average fines content (F), and median grain size (d_{50}) of the interval with $(N_1)_{60}<15$.

For a free face:

$$\log (D+0.01) = -16.366 + 1.178 M_w - 0.927 \log R - 0.013 R + 0.657 \log W + 0.348 \log H + 4.527 \log (100 - F) - 0.922 d_{50} \quad (4)$$

For sloping ground:

$$\log (D+0.01) = -15.787 + 1.178 M_w - 0.927 \log R - 0.013 R + 0.429 \log \theta + 0.348 \log H + 4.527 \log (100 - F) - 0.922 d_{50} \quad (5)$$

Horizontal displacements predicted by equations (1) to (5) are shown in Table 2. All of the predictive methods overestimate observed displacements at Miller Farm

Changes of Elevation

We used the simplified method of Tokimatsu and Seed (1987) to predict settlement from post-liquefaction consolidation at 3 SPT/CPT locations at Miller Farm (Table 3). Unfortunately,

only one SPT/CPT sounding, no. 5, is within the area of the post-earthquake topographic survey. Thus, a direct comparison only can be made at this location. At this location where 100 mm of settlement was observed, we predict only 25 mm of settlement. The other borings, although on the lateral spread, are only useful for predicting the general magnitude of settlement. Predicted settlements at Miller Farm ranged from 20 to 80 mm.

The method uses induced cyclic stress ratio and $(N_1)_{60}$ to predict post-liquefaction strain. Settlement is estimated by multiplying the predicted strain by sand-layer thickness, which we determined from the CPT sounding. Because the method was developed for clean sands, a correction should be applied to account for the effect of fines in diminishing post-liquefaction consolidation. Following the procedure suggested by O'Rourke and others (1991), we increased $(N_1)_{60}$ to account for the influence of fines content. Predicted settlements for both clean sand and sand with corrections for fines content are shown in Table 3.

MECHANISM OF HORIZONTAL GROUND DEFORMATION

Because horizontal displacements were small and the boundary between younger and older flood-plain deposits may be sharp and nearly vertical, we considered the possibility that the observed horizontal displacements were caused by differential vertical displacement at depth. By this mechanism, surficial horizontal displacements were caused by bending of the overburden when differential post-liquefaction consolidation occurred beneath the overburden and across the nearly vertical boundary between the liquefied and nonliquefied zones. No horizontal deformation in the liquefied zone was assumed. We analyzed this mechanism by treating the overburden as an elastic beam subject to differential displacements along its base. Lee and Shen (1969) proposed that horizontal displacement (D) can be estimated by:

$$D = \tfrac{2}{3} T \alpha \qquad (6)$$

where T is the thickness of the overburden and α is the change in slope of the land surface. For a T = 4.6 m and a change in slope of approximately 0.0083 (Fig. 9), equation (6) predicts only about 25 mm of horizontal displacement, which is 16-21% of the observed displacement Thus, we conclude that horizontal deformation within the liquefied zone was the primary cause of horizontal surface displacement.

A flow failure mechanism for the lateral spread is inconsistent with the pre-earthquake land slopes at Miller Farm provided by the land owner. Land in the western part of the Miller Farm portion of the lateral spread sloped at 0.264% away from the river (Fig. 1). If this slope is valid, and we have no evidence to the contrary, the western part of the lateral spread should have moved away from the channel. Field observations indicated that displacement was channelward. The eyewitness accounts of continued venting from sand boils after the earthquake also are inconsistent with a flow failure. Continued venting implies pore pressures remained elevated which are conducive to large ground displacements.

We also considered the possibility that the flow failure was driven by static stresses associated with the topographic relief of the river channel. When the lateral spread is examined at true scale (Fig. 5B), however, it is unlikely that these stresses would be significant as far away

from the channel as the head scarp. Thus, a progressive failure would be required for these stresses to be the cause of the flow failure. Such a failure is not supported by the field observations that indicated the block remained essentially intact.

To evaluate the feasibility of a deformation failure, we performed a Newmark (1965) sliding block analysis using the Watsonville strong ground motion record for loading. We assumed the failure surface was in the upper part of the liquefied zone because blow counts are lower in this zone and most of the sand boils appear to have been derived from this zone (Fig. 3). A deeper sliding surface also would involve passive resistance of soil beneath the river channel (Fig. 5) which would imply that failure is not occurring on the plane of least resistance Back-calculated residual strengths for such a failure ranged from 7 to 9 kPa for failure surfaces with slopes ranging from 0.05 to 0.7 degrees. These values of residual strength are consistent with residual strengths inferred from observed corrected blow counts using the correlation by Seed and Harder (1990).

Because both the failure surface and the residual strength of the liquefied soil were uncertain, we devised a method to estimate the maximum possible permanent displacement in a deformation failure. The method requires a nearby strong motion record. The method rests on the assumption that the mechanism for deformation failure is that the lateral spread behaves as a block that is detached from the underlying soil by the liquefied zone and can only move relative to the failure surface in the downslope direction. During cyclic loading, the block cannot keep pace with the underlying soil during upslope dynamic displacements because of the reduction in strength along its base. Hence, relative, but permanent, downslope displacement occurs. During downslope dynamic displacements, the block and underlying soil move together and no relative displacement occurs. The maximum permanent ground deformation then is the summation of the peak-to-peak displacements, calculated by double integration of the acceleration time history, in the upslope direction (Fig. 6). For the Watsonville record, the sum of the peak-to-peak displacements in the southeast direction is 1,156 mm, which is approximately 7 times the observed permanent displacement at Miller Farm, 160 mm, and 3 times the maximum observed displacement on the spread, 300 mm. This implies that ground displacements during the mainshock were large enough to cause the observed permanent horizontal displacements by a sliding block model

SURFACE MANIFESTATIONS OF LIQUEFACTION

Our observations at Miller and Farris Farms are consistent with the compilation by Ishihara (1985) that describes the conditions under which surface damage from liquefaction is observed. Ishihara (1985) correlated thicknesses of the liquefied layer with the nonliquefied surface layer for areas with and without surface effects for different accelerations. The data point for both farms falls well within the part of his graph where surface manifestations of liquefaction are observed (Fig. 10).

CONCLUSIONS

The 1.7-km-long Miller Farm lateral spread was the largest lateral spread caused by the Loma Prieta earthquake. Empirical methods for predicting horizontal displacement overestimate observed displacements by as much as an order of magnitude. The best predictions are by Bartlett and Youd (1992). Settlements are underestimated by empirical methods. Observed displacements and soil properties are consistent with an inertial deformation failure mechanism. A flow failure mechanism is unlikely because the ground moved opposite to land slope in parts of the lateral spread.

ACKNOWLEDGMENTS

We gratefully acknowledge the help of the following people and organizations that made this investigation possible. Clint Miller Farms and the family of Marie K. Farris permitted access to the land on which we worked. Granite Construction Company and Pacific Bell allowed us to locate portable seismographs at their facilities. J. Hamilton conducted the post-earthquake survey at Miller Farm. C. Criley assisted in drilling and analyzing SPT samples. S.D. Ellen and K.H. Chang measured the profile of ground displacements across the lateral spread. The California Strong Motion Instrumentation Program provided the Watsonville accelerograms. S. Toprak and T.D. O'Rourke performed the Newmark analysis. M. G. Bonilla and R.E. Kayen reviewed drafts of the manuscript. We particularly appreciate the insightful discussions about the Newmark analysis with T.D. O'Rourke, M. Palmer, J. Pease, and H.E. Stewart.

REFERENCES

Bartlett, S. F., and Youd, T. L., 1992, Empirical prediction of lateral spread displacement, *in* Proceedings, 4th U.S.-Japan workshop on earthquake resistant design of lifeline facilities and countermeasures for soil liquefaction, NCEER-92-0019, National Center for Earthquake Engineering Research, Buffalo, p. 351-363.

Dupré, W. R., and Tinsley, J. C., III, 1980, Maps showing geology and liquefaction potential of northern Monterey and southern Santa Cruz Counties, California: U.S. Geological Survey, Miscellaneous Field Studies Map MF-1199 (scale 1:62,500).

Hamada, M., 1992, Large ground displacements and their effects on lifelines - 1964 Niigata earthquake *in* Case Histories of Liquefaction and Lifeline Performance during past Earthquakes: v. 1: Japanese Case Studies, M. Hamada and T.D. O'Rourke, eds., NCEER-92-0001, National Center for Earthquake Engineering Research, Buffalo, p. 3-1 to 3-123.

Hamada, M., Yasuda, S., Isoyama, R , and Emoto, K., 1986, Study of liquefaction induced permanent ground displacements: Association for the Development of Earthquake Prediction, Tokyo, 87 p.

Ishihara, K., 1985, Stability of natural deposits during earthquakes, *in* 11th International Conference on Soil Mechanics and Foundation Engineering, San Francisco, p. 321-376.

Lee, K. L., and Shen, C. K., 1969, Horizontal movements related to subsidence: Journal of Geotechnical Engineering, ASCE, v. 95, no. 1, p. 139-166.

National Research Council, 1985, Liquefaction of soils during earthquakes: National Academy Press, Washington, D.C., 240 p.

Newmark, N. M., 1965, Effects of earthquakes on dams and embankments: Geotechnique, v. 15, p. 139-159.

O'Rourke, T. D., Gowdy, T. E., Stewart, H. E., and Pease, J. W., 1991, Lifeline performance and ground deformation in the Marina during 1989 Loma Prieta earthquake, *in* Proceedings, 3rd U.S.-Japan workshop on earthquake resistant design of lifeline facilities and countermeasures for soil liquefaction, NCEER-91-0001, National Center for Earthquake Engineering, Buffalo, p. 129-146.

Pease, J. W., and O'Rourke, T. D., 1993, Liquefaction hazards in the Mission District and South of Market Street areas, San Francisco, California: U.S. Geological Survey, External Contract No. 14-08-0001-G2128.

Seed, H. B., Tokimatsu, K., Harder, L. F., and Chung, R. M., 1985, Influence of SPT procedures in soil liquefaction resistance evaluation: Journal of Geotechnical Engineering, ASCE, v. 111, no. 12, p. 1425-1445.

Seed, R. B., and Harder, L. F., Jr., 1990, SPT-based analysis of cyclic pore pressure generation and undrained residual strength, *in* Duncan, J. M., ed., H. Bolton Seed: Vancouver, B.C., BiTech Publishers Limited, p 351-376.

Shakal, A., Huang, M., Reichle, M., Ventura, C., Cao, T., Sherburne, R., Savage, M., Darragh, R., and Petersen, C., 1989, CSMIP strong-motion records from the Santa Cruz Mountains (Loma Prieta), California earthquake of 17 October 1989: California Strong Motion Instrumentation Program Report no. OSMS 89-06, p. 57.

Tinsley, J. C., III, and Dupré, W. R., 1992, Liquefaction hazard mapping, depositional facies, and lateral spreading ground failure in the Monterey Bay area during the 10/17/89 Loma Prieta earthquake, *in* Proceedings, 4th U.S.-Japan workshop on earthquake resistant design of lifeline facilities and countermeasures for soil liquefaction, NCEER-92-0019, National Center for Earthquake Engineering Research, Buffalo, p. 71-85.

Tokimatsu, K., and Seed, H. B., 1987, Evaluation of settlements in sand due to earthquake shaking: Journal of Geotechnical Engineering, ASCE, v. 113, no. 8, p. 861-878.

Youd, T. L., and Perkins, D. M., 1987, Mapping of liquefaction severity index: Journal of Geotechnical Engineering, ASCE, v. 113, no. 11, p. 1374-1392.

Table 1. Geotechnical properties of liquefied layer

Property	Miller Farm	Farris Farm	Combined
Thickness	6.1 m	6.1 m	6.1 m
Fines content	22 %	8 %	15 %
d_{50}	0.16 mm	0.21 mm	0.19 mm
$(N_1)_{60}$	14±7	18±6	16±7

Table 2. Predicted and observed horizontal displacements

Method	Displacement, mm
Hamada and others (1986)	1,040
Pease and O'Rourke (1993)	2,120
Youd and Perkins (1987)	990
Bartlett and Youd (1992)	
Free face	600
Sloping ground	540
Observed	**117 to 160**

Table 3. Predicted settlements

Sounding	Sand layer thickness, m	Predicted Settlement, mm		**Observed Settlement, mm**
		Clean sand	Fines corrected	
3	2.0	30	20	
5	5.2	61	25	**100**
8	6.2	113	80	

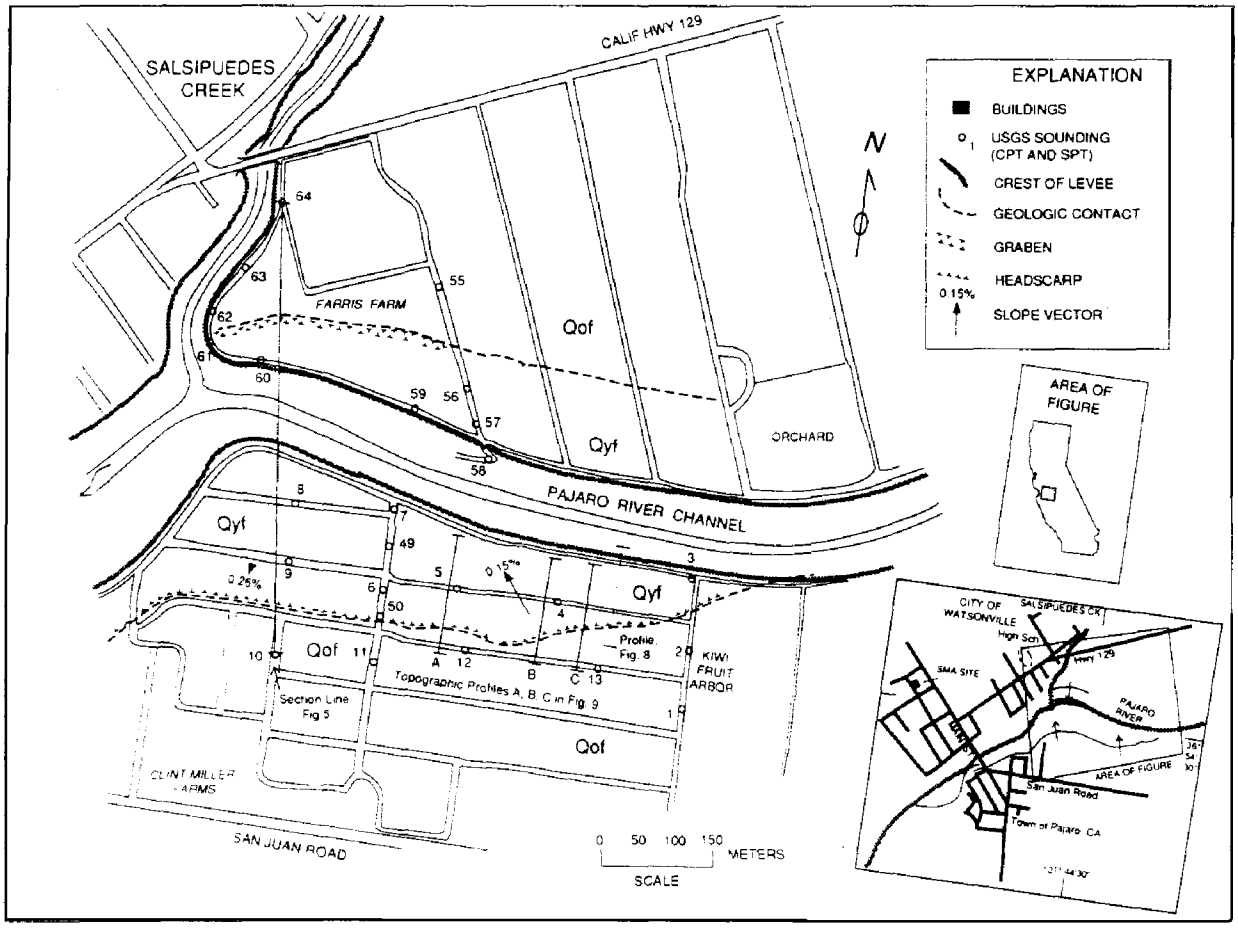

Fig. 1 Map of Miller and Farris Farms showing the lateral spread and locations of soundings and profiles. Arrows at Miller Farm indicate pre-earthquake slope from grading specifications reported by landowner. Map units Q_{yf} and Q_{of} are younger and older flood-plain deposits, respectively (Dupré and Tinsley, 1980).

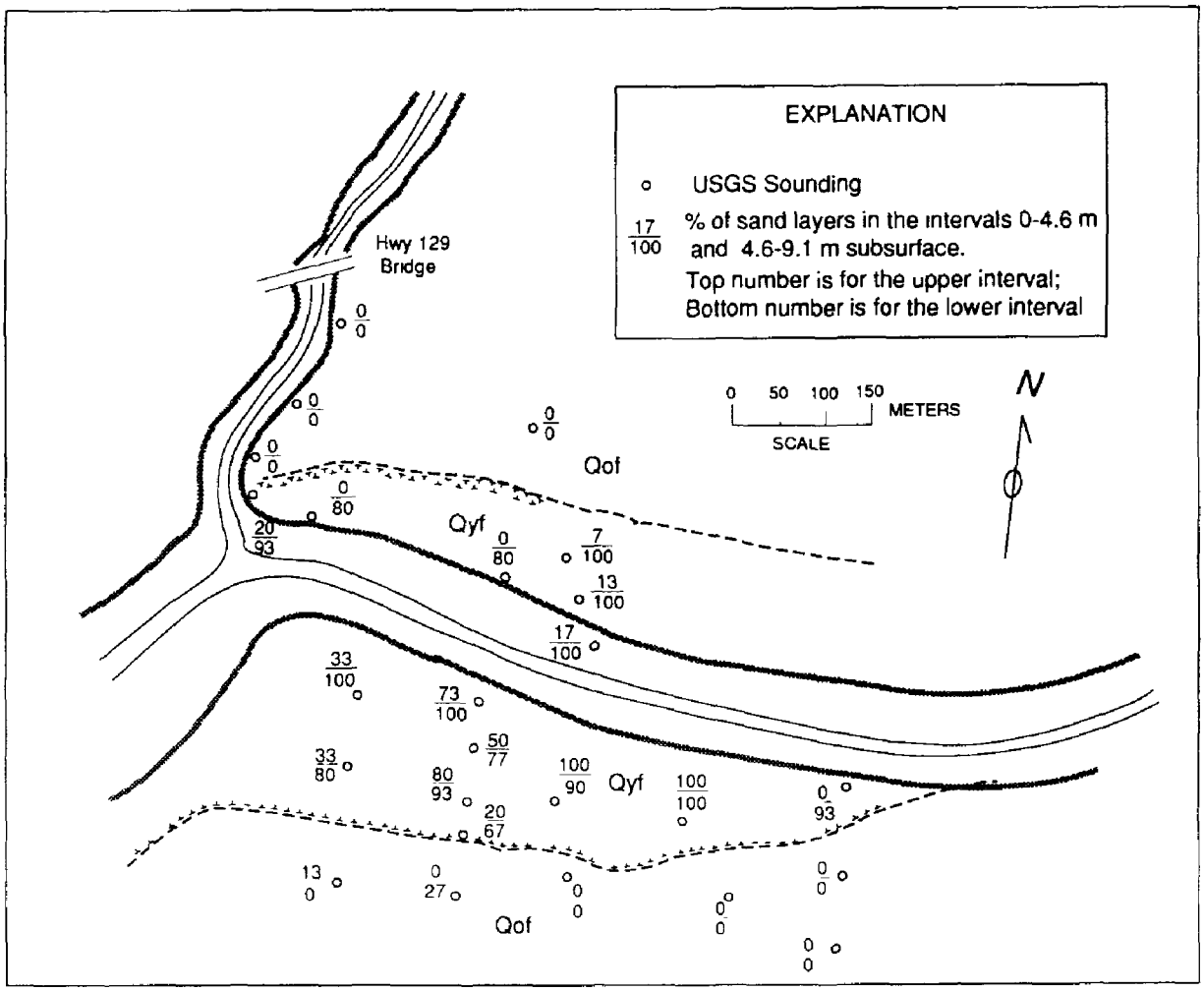

Fig. 2 Map of sandy layers as a percentage of interval thickness for depth intervals 0 to 4.6 m and 4.6 to 9.1 m. Upper and lower values are for upper and lower depth intervals, respectively.

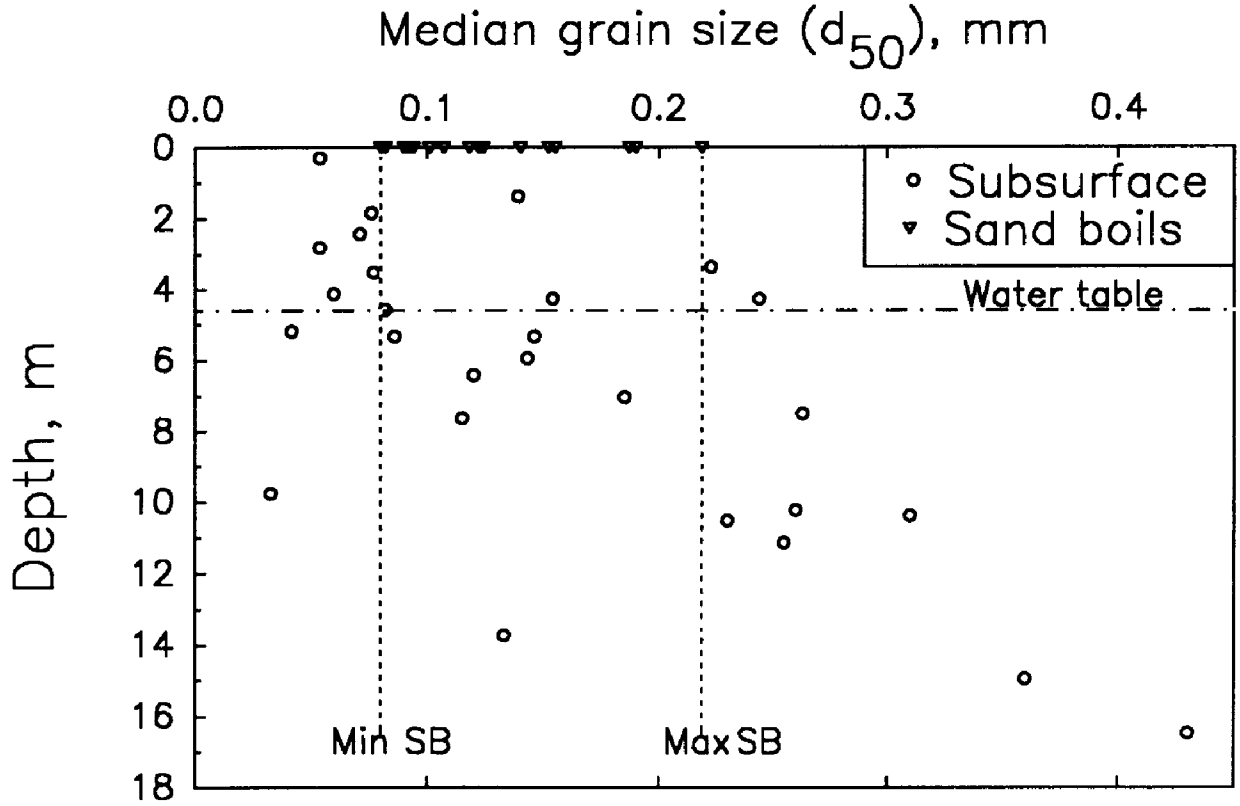

Fig. 3 Median grain size, d_{50}, as function of depth for Miller Farm. Inverted triangles show d_{50} of sand boils. Min SB and Max SB are the minimum and maximum d_{50} of sand boils, respectively.

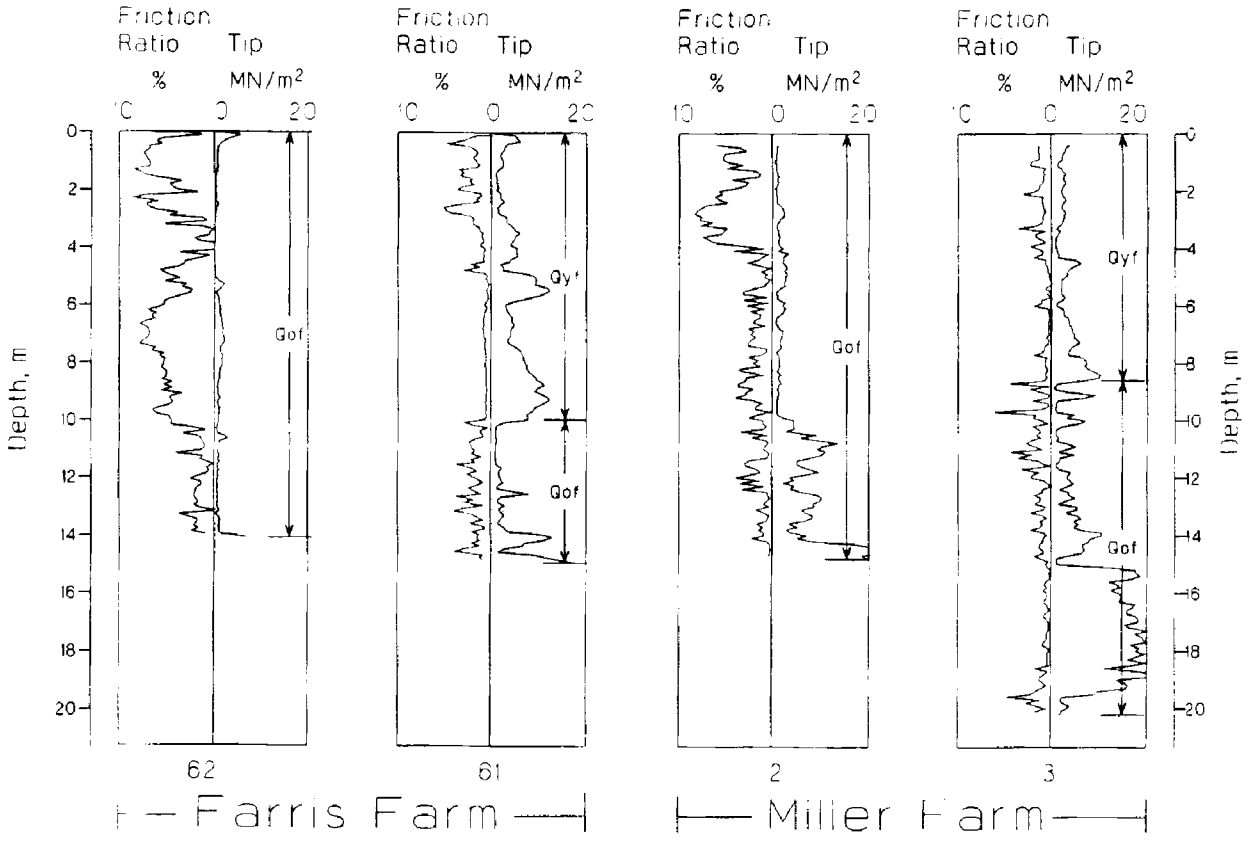

Fig. 4 Comparison of closely spaced cone penetration tests that straddle the contact between older (Q_{of}) and younger (Q_{yf}) flood-plain deposits at Farris and Miller Farms. See Figure 1 for locations.

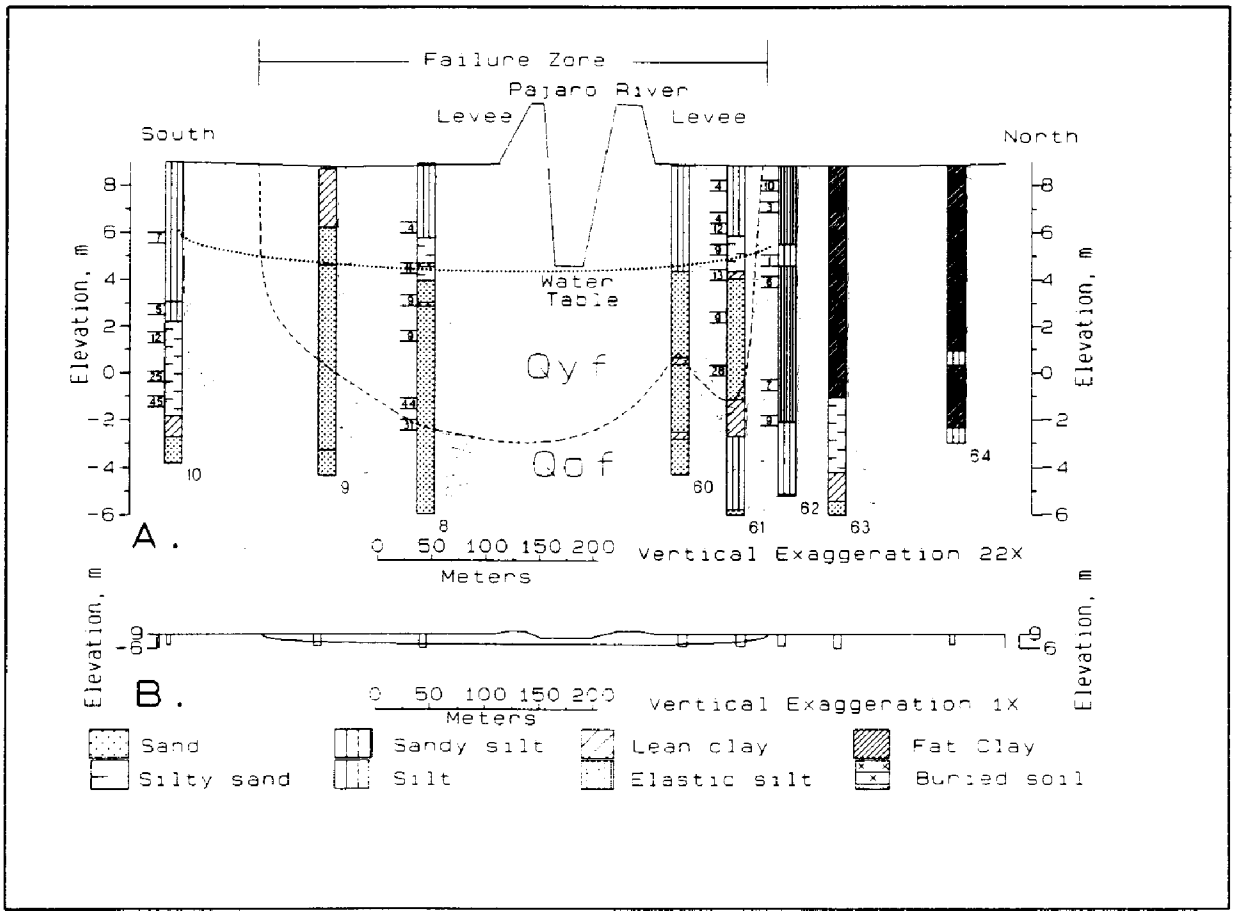

Fig. 5 Geologic cross section of the buried river channel at exaggerated (A) and true (B) scale. Curves to the right of the soundings are CPT tip resistance; numbers to the left are SPT field blow counts in blows/foot. Sounding number is shown at base of log. See Figure 1 for location.

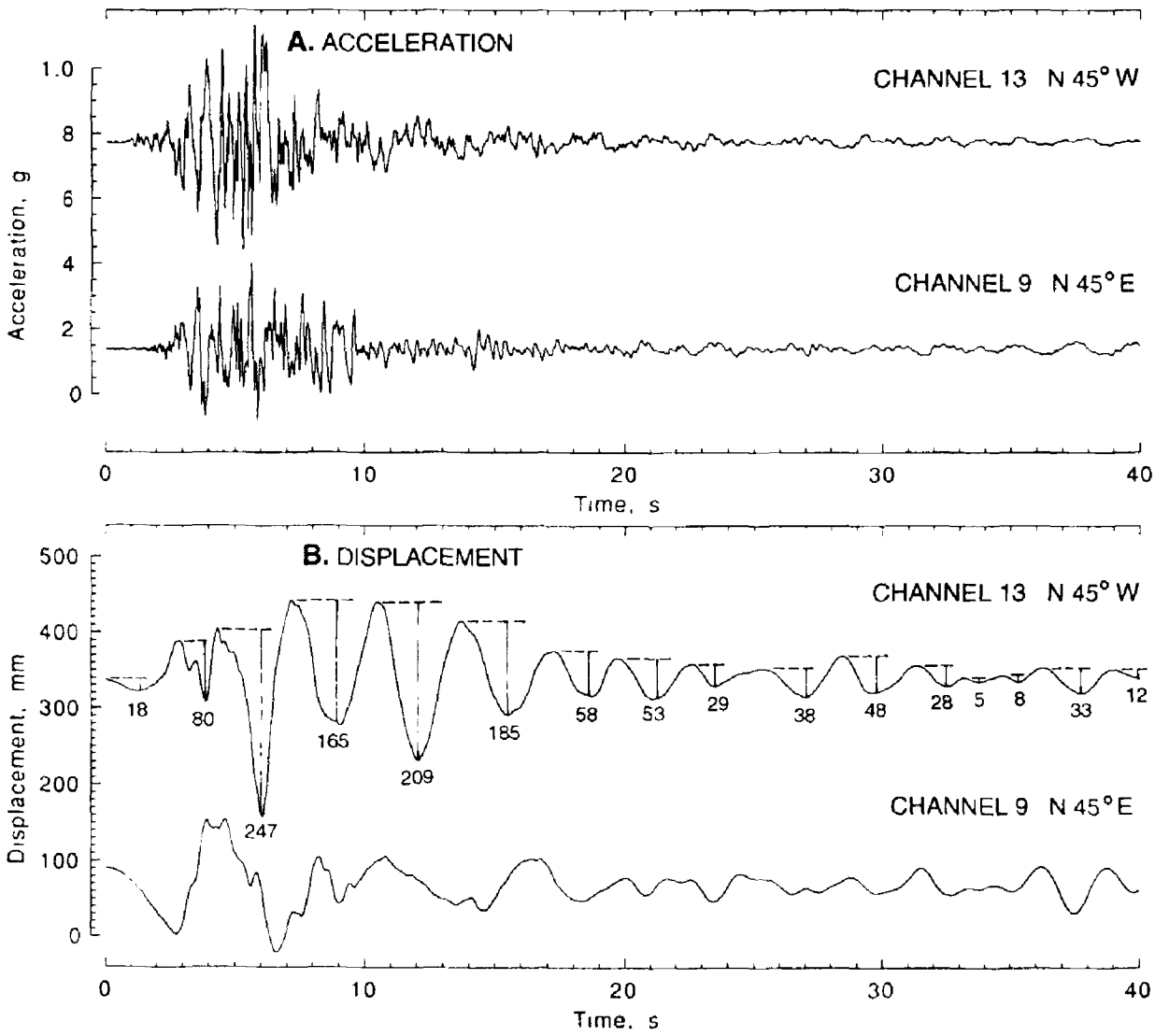

Fig. 6 A. Accelerograms of Loma Prieta earthquake mainshock recorded by orthogonal horizontal accelerometers at ground level in phone company building at Watsonville (the azimuth is the direction of positive acceleration); B. Displacements computed by double integration of acceleration time history. Peak-to-peak displacement, in mm, is shown for channel 13. Total of peak-to-peak displacements equals 1,156 mm. See SMA site in insert in Figure 1 for location.

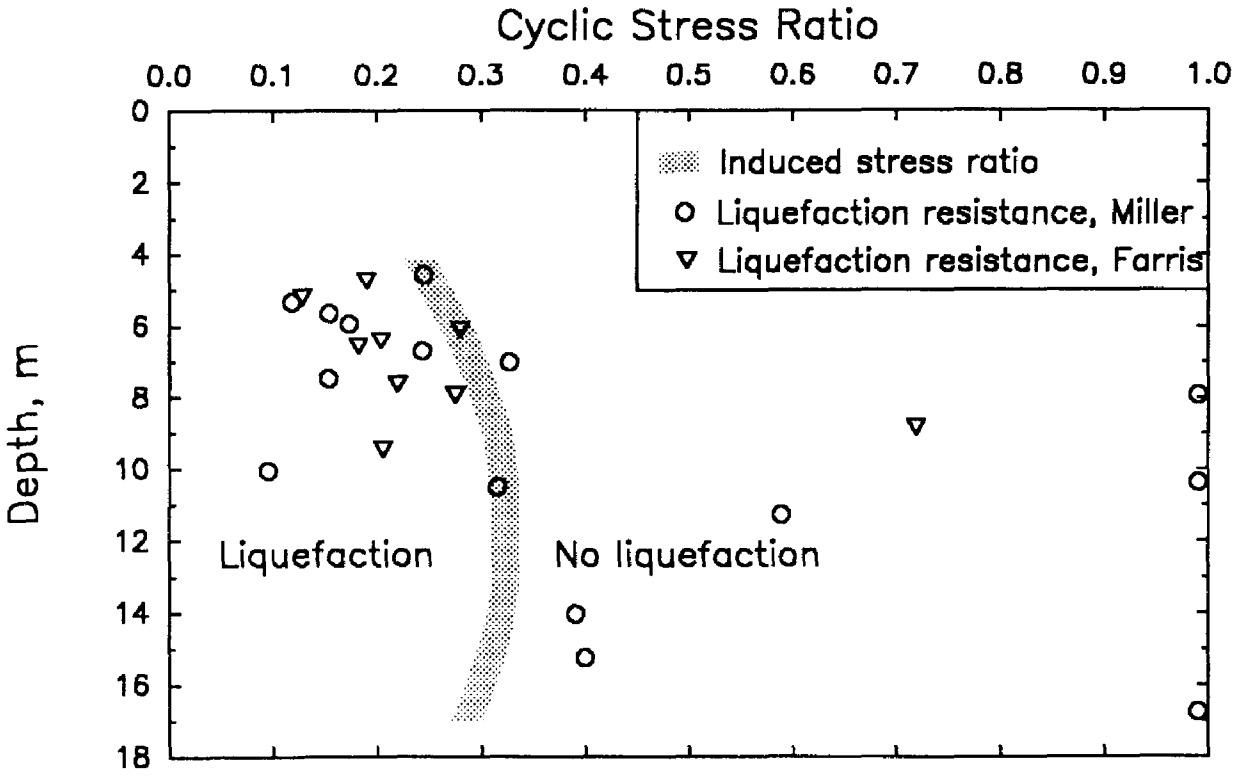

Fig. 7 Comparison of induced stress ratio with the stress ratio required to liquefy as a function of depth for SPT soundings at Miller and Farris Farms. Stress ratios shown as 0.99 are actually much greater than one.

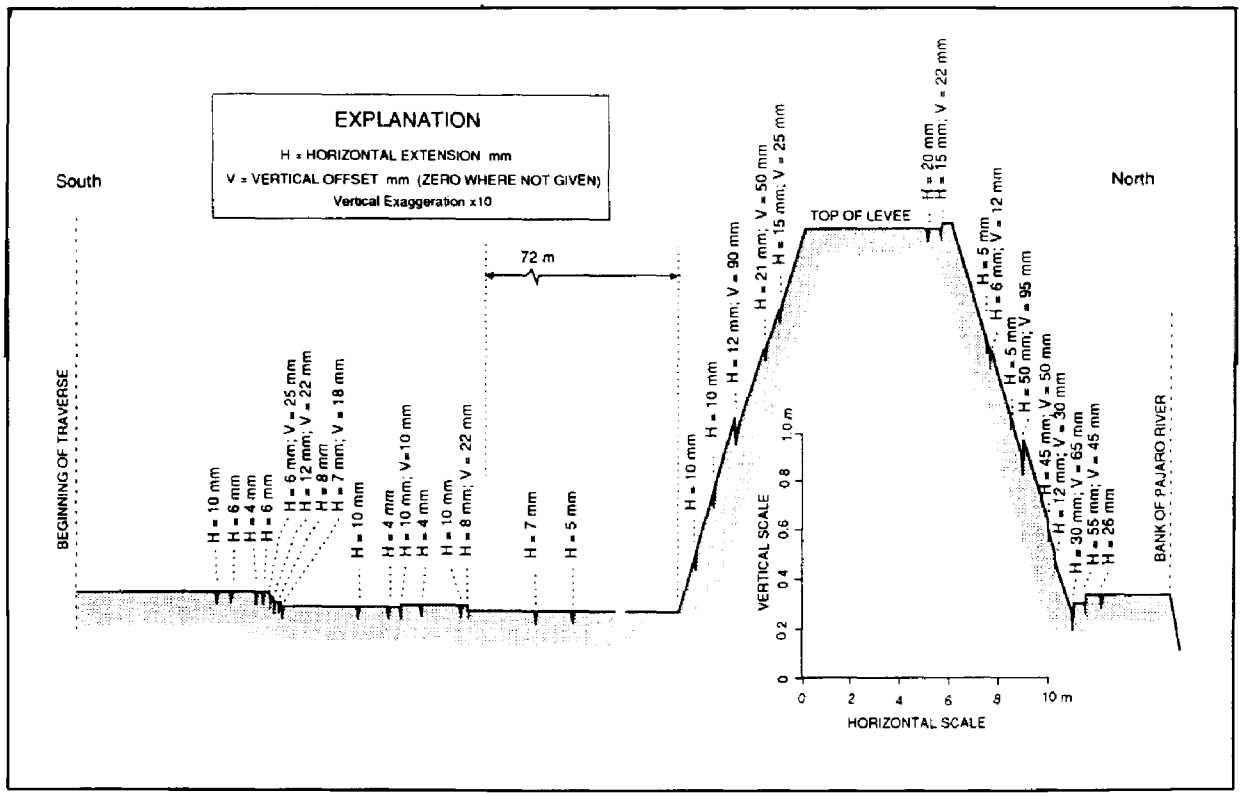

Fig. 8 Vertical offset and horizontal opening across ground cracks at Miller Farm. See Figure 1 for location.

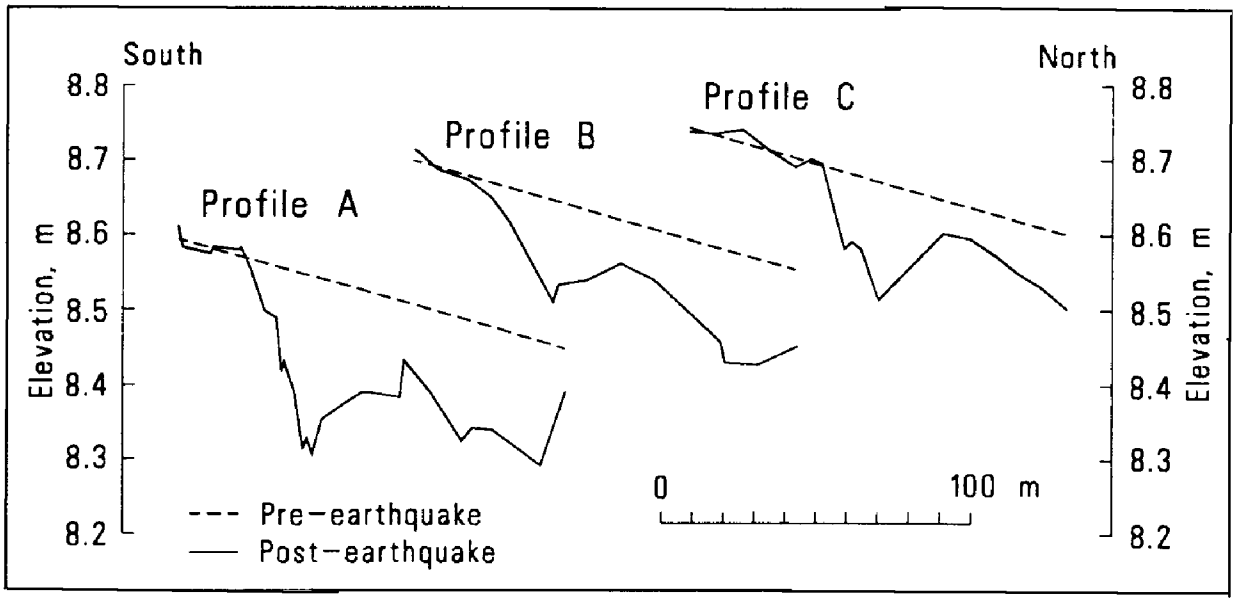

Fig. 9 Pre- and post-earthquake profiles of the land surface on Miller Farm. See Figure 1 for locations.

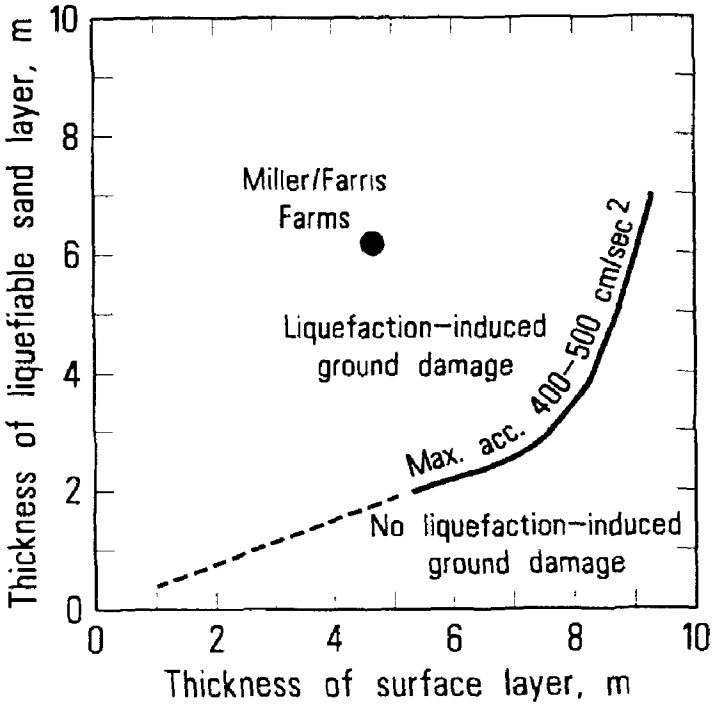

Fig. 10 Comparison of observation at Miller/Farris Farms to Ishihara's (1985) correlation of observation of liquefaction effects with thicknesses of liquefied layer and nonliquefied surficial layer.